Live cell screening identifies glycosides as enhancers of cardiomyocyte cell cycle activity

Ajit Magadum[1,2,3]*, Harsha V. Renikunta[1,4], Neha Singh[5], Conchi Estaras[3], Raj Kishore[3,6] and Felix B. Engel[1,7,8]*

[1]Department of Cardiac Development and Remodelling, Max-Planck-Institute for Heart and Lung Research, Bad Nauheim, Germany, [2]Cardiovascular Research Center, Icahn School of Medicine at Mount Sinai, New York, NY, United States, [3]Lewis Katz School of Medicine, Center for Translational Medicine, Temple University, Philadelphia, PA, United States, [4]Department of Cardiology, Charité Berlin - University Medicine, Berlin, Germany, [5]Department of Sports Biosciences, Central University of Rajasthan, Ajmer, India, [6]Department of Cardiovascular Sciences, Lewis Katz School of Medicine at Temple University, Philadelphia, PA, United States, [7]Experimental Renal and Cardiovascular Research, Department of Nephropathology, Institute of Pathology, Friedrich-Alexander-Universität Erlangen-Nürnberg (FAU), Erlangen, Germany, [8]Muscle Research Center Erlangen (MURCE), Erlangen, Germany

Promoting cardiomyocyte proliferation is a promising strategy to regenerate the heart. Yet, so far, it is poorly understood how cardiomyocyte proliferation is regulated, and no factor identified to promote mammalian cardiomyocyte proliferation has been translated into medical practice. Therefore, finding a novel factor will be vital. Here, we established a live cell screening based on mouse embryonic stem cell-derived cardiomyocytes expressing a non-functional human geminin deletion mutant fused to Azami Green (CM7/1-hgem-derived cardiomyocytes). We screened for a subset of compounds of the small molecule library Spectrum Collection and identified 19 potential inducers of stem cell-derived cardiomyocyte proliferation. Furthermore, the pro-proliferative potential of identified candidate compounds was validated in neonatal and adult rat cardiomyocytes as well as human induced pluripotent stem cell-derived cardiomyocytes. 18 of these compounds promoted mitosis and cytokinesis in neonatal rat cardiomyocytes. Among the top four candidates were two cardiac glycosides, peruvoside and convallatoxin, the flavonoid osajin, and the selective α-adrenoceptor antagonist and imidazoline I1 receptor ligand efaroxan hydrochloride. Inhibition of PTEN and GSK-3β enhanced cell cycle re-entry and progression upon stimulation with cardiac glycosides and osajin, while inhibition of IP3 receptors inhibited the cell cycle-promoting effect of cardiac glycosides. Collectively, we established a screening system and identified potential compounds to promote cardiomyocyte proliferation. Our data suggest that modulation of calcium handling and metabolism promotes cardiomyocyte proliferation, and cardiac glycosides might, besides increasing myocardial contraction force, contribute to cardiac repair by inducing cardiomyocyte proliferation.

KEYWORDS

cardiac glycosides, cardiomyocyte proliferation, calcium handling, live cell screening platform AG, Azami Green, stem cell, small molecules, cell cycle

Introduction

Heart failure remains a major socio-economic challenge. Despite significant achievements in medical practice resulting in reduced acute mortality of myocardial infarction (MI), the prevalence of heart failure is increasing (1). Thus, there is a great need to develop strategies that allow to increase the muscle mass of the heart to enhance heart function. In recent years, induction of cardiomyocyte proliferation has been proposed as an important approach for cardiac regeneration (2). An alternative is cardiac tissue engineering. Also in this context, induction of proliferation of stem cell-derived cardiomyocytes is of interest, for example, to enable the generation of compact cardiac tissues during biofabrication (3–5).

Human cardiac regeneration is limited due to low postnatal cardiomyocyte replicative rates as well as progressive polyploidization (2, 6). The mechanism underlying the establishment of the cell cycle arrest in mammalian cardiomyocytes remains poorly understood. Recently, several mechanisms have been suggested including sarcomere formation (7–9), cyclin G1 expression (10), heterochromatin formation (11), loss of centrosome integrity (12), as well as metabolic switch (13, 14). In addition, while initially very few factors were identified to induce significant cardiomyocyte proliferation, in the last decade, a large number of stimuli have been reported to induce cardiomyocyte proliferation and heart regeneration (2, 15–17). Yet, none of these factors has so far been translated into medical practice.

Here, we have applied a chemical approach to modulate proliferation of stem cell-derived cardiomyocytes, which has several advantages over conventional genetic methods such

---

Abbreviations: AG, Azami Green; ANOVA, analysis of variance; ara C, cytosine-D-arabinofuranoside; BIO, 6-bromoindirubin-3'-oxime; BrdU, 5-Bromo-2-deoxyuridine; cdc2, cyclin dependent kinase 1; cDNA, complementary deoxyribonucleic acid; DAPI, 4', 6'-diamidino-2-phenylindole; DMEM, Dulbecco's Modified Eagle Medium; DMSO, Dimethylsulfoxid; DNA, deoxyribonucleic acid; EB, embryoid bodies; ES, embryonic stem; FASN, fatty acid synthase; FBS, fetal bovine serum; flk1, fetal liver kinase 1; FGF1, fibroblast growth factor 1; gapdh, glyceraldehyde-3-phosphate dehydrogenase; GSK-3, glycogen synthase kinase-3; H3P, histone H3 phosphorylation on serine10; hiPSC, human induced pluripotent stem cells; IP3, inositol trisphosphate; LIF, leukemia inhibitory factor; mAG-hGem(1/110), non-functional human geminin deletion mutant fused to a monomeric version of AG; MI, myocardial infarction; myh7, myosin heavy chain 7; nkx2-5, NK2 homeobox 5; oct, octamer binding transcription factor; P3, 3-day-old; p38i, mitogen-activated protein kinase inhibitor SB203580; PBS, phosphate-buffered saline; PI3K, phosphoinositide 3-kinase; PPAR, peroxisome proliferator-activated receptor; PTEN, phosphatase and tensin homolog; RNA, ribonucleic acid; RT-PCR, reverse transcription followed by polymerase chain reaction; SEM, standard error of the mean.

---

as enabling temporal control, rapid inhibition or activation, regulation of functionally overlapping targets, and applicability of the identified chemicals across similar species. Notably, many chemicals can be applied directly as therapeutic drugs. In addition, we have established a Fucci-based (18) live cell screening, which eliminates the need for techniques such as immunofluorescence staining, incorporation of nucleotide analogs, or cell count assays. In addition, a live cell screening can capture events that may develop at different times post-treatment, which may be potentially overlooked by end-point assays. Screening of over 700 compounds and validation in primary cardiomyocytes identified as the four most potent promotors of cardiomyocyte cell cycle progression two cardiac glycosides, peruvoside and convallatoxin, the flavonoid osajin, and the selective α-adrenoceptor antagonist and imidazoline I1 receptor ligand efaroxan hydrochloride. To date, no study reports that any of these four compounds have an effect on cardiomyocyte cell cycle progression or heart regeneration.

Cardiac glycosides are a group of compounds, which are secondary metabolites produced by certain plants, insects, and vertebrates. They are mainly known as inhibitors of the sodium-potassium pump in eukaryotic cells and are used as drugs to treat heart disease (e.g., cardiac arrhythmia, congestive heart failure, and atrial fibrillation) by increasing myocardial contraction force and, at the same time, lowering the frequency of this contraction (19–21). Interestingly, data are accumulating which indicate that cardiac glycosides have additional targets such as the nuclear receptor superfamily of transcription factors (19). However, their toxicity prevents their widespread use, and thus a better understanding of the function of cardiac glycosides is necessary (20).

Methods

Isolation of primary cardiomyocytes

The investigation conforms with the guidelines from Directive 2010/63/EU of the European Parliament on the protection of animals used for scientific purposes. Extraction of organs and preparation of primary cell cultures were approved by the local Animal Ethics Committee in accordance with governmental and international guidelines on animal experimentation (protocol TS-9/2016 Nephropatho). Ventricular cardiomyocytes from 3-day-old (P3) and 12-week-old (adult) Sprague Dawley rats were isolated and cultured as described (22). Rats were first injected s.c. with 0.04 mg/kg buprenorphine and were anesthetized after 30 min by isoflurane inhalation (2 ml vaporized in a 5 l beaker). After loss of standing, eyelid and pedal reflexes, animals were sacrificed by exsanguination due to heart excision upon thoracotomy. Hearts from P3 rats were dissected upon decapitation with operating scissors (ROBOZ [RS-6845], no anesthesia), base

with atria removed, and the remaining ventricle minced. Cells were initially cultured for 48–72 h in the presence of 20 μM cytosine-D-arabinofuranoside (ara C) and 5% horse serum before stimulation to prevent non-myocyte proliferation. Cardiomyocytes were subsequently treated in the presence of fetal bovine serum (FBS) (neonatal: 0.2% FBS; adult: 0.5% FBS: adult) as indicated. Postnatal cardiomyocytes were stimulated once; adult cardiomyocytes every day.

Reagents

The chemical reagents and recombinant proteins were obtained from different companies: "Spectrum Collection" (MicroSource Discovery Systems, Inc., 10 mM stock solutions in dimethylsulfoxid (DMSO), purity > 90%), 6-bromoindirubin-3'-oxime (BIO), osajin, peruvotoxin, efaroxan hydrochloride, xestospongin C (Tocris bioscience), SB203580 (Calbiochem), fibroblast growth factor 1 (FGF1, R&D Systems), convallatoxin (Sigma), valeryl salicylate, bpV(HOpic) (Santa Cruz Biotechnology). Inhibitors were added 1 h before cardiomyocyte stimulation.

Generation of CM7/1-hgem mouse stem cell line

The mouse embryonic stem (ES) cell line CM7/1 (23) was cultured in stem cell medium [DMEM containing 2 mM L-glutamine (GIBCO), penicillin (100 U/mL), streptomycin (100 μg/mL) (Sigma), beta-mercaptoethanol (Merck), 3 mM Na-pyruvate (Thermo Fisher), and 15% FBS (PAA Laboratories)] for 2 days in the presence of leukemia inhibitory factor (LIF, Sigma). The cells were transfected with linear mAG-hGem (1/110) plasmid (18) using lipofectamine 2000 (Thermo Fisher). After 48 h, cells were selected for utilizing 200 μM Zeocin antibiotic (Thermo Fisher) for 2 weeks. Single growing colonies were selected and expanded, resulting in several cell lines. One of the cell lines showing Azami Green (AG) expression was differentiated into beating embryoid bodies (Ebs) and then dissociated into cardiomyocytes. This mouse stem cell line was called CM7/1-hgem and was used in this study.

Differentiation of CM7/1-hgem mouse stem cell line

CM7/1-hgem ES cells were cultured in stem cell medium for 2 days in the presence of LIF (Sigma). The cells were trypsinized with 0.005% trypsin (GIBCO) and counted by hemocytometer. For differentiation, 330,000 cells/ 10 ml differentiation medium (Dulbecco's Modified Eagle Medium (DMEM) containing 2 mM

L-glutamine, penicillin (100 U/mL), streptomycin (100 μg/mL), and 3 mM Na-pyruvate, 10% FBS) were used for the hanging drop method. After 2 days, formed Ebs were transferred to suspension culture (10 cm cell culture plate) containing differentiation medium. The plates were stirred at 50 rpm. On day 9, when Ebs started to beat, differentiation medium was replaced with differentiation medium containing 400 μM G418 (Thermo Fisher) to eliminate non-myocytes. After 4–5 days, Ebs were dissociated with 1 mM collagenase B (Sigma) in phosphate-buffered saline (PBS) and centrifuged at 400 RCF for 5 min. Subsequently, single cells were seeded on fibronectin-coated cell culture plates (15,000 cells/well) in cardiomyocyte medium (DMEM containing 2 mM L-glutamine, penicillin (100 U/mL), streptomycin (100 μg/mL), and 3 mM Na-pyruvate, 0.2% FBS) and 400 μM G418 (100 μl/well) and cultured for 5 to 6 days. Then, cells were washed and treated with small molecules utilizing a cardiomyocyte medium.

Screening

CM7/1-hgem-derived cells were treated once with the indicated compounds at a concentration of 1 μM. More than 700 molecules were screened from the bioactive collection of the "Spectrum Collection" from MicroSource Discovery Systems, Inc. (Gaylordsville, CT) (Supplementary Table 1). We used cardiomyocyte medium with DMSO as negative control and 10% FBS and FGF1 + p38 mitogen-activated protein kinase inhibitor SB203580 (FGF1/p38i) as positive controls. AG expression was analyzed every 12 h (for quantitative analysis, around 100 cells were evaluated) for the following 4 days by visual inspection using a Leica fluorescence microscope. The maximal number of mAG-hGem(1/110)-positive cells were used to normalize the data against the DMSO-treated control as a fold-change. Hit compounds were defined as those giving an effect higher than 2-fold. Individual samples of hit compounds were picked from the original library and confirmed with the same method as in the primary screen for three times.

Reverse transcription followed by polymerase chain reaction (RT-PCR) analysis

Total ribonucleic acid (RNA) was isolated from Ebs derived from CM7/1-hgem mouse stem cells at different time points using the Rneasy Kit (Qiagen). The cDNA (complementary deoxyribonucleic acid) was prepared from isolated RNA using *MMLV* or superscript II reverse transcriptase and the oligo(dT) primer (Qiagen). PCR was performed according to standard protocols (Applied Biosystems). Primers: *octamer binding transcription factor* (*oct*)*3/4*: forward (F) 5′-TGAGAACCTTCA

GGAGATATGCAA — 3′,reverse©,5′-CTCAATGCTAGTTCG CTTTCTCTTC — 3′,nanog:F5′-AGTATCCCAGCATCCATTG C — 3′,R,5′-TTTCACCTGGTGGAGTCACA — 3′,brachyury:F 5′-CTCCAACCTATGCGGACAAT — 3′,R,5′-CCCCTTCATA CATCGGAGAA — 3′,isl1:F5′-GCGACATAGATCAGCCTGC T — 3′,R,5′-GTGTATCTGGGAGCTGCGAG — 3′,fetalliverkin ase1(flk1):F5′-GGGTTTGGTTTTGGAAGGTT-3′,R,5′-AGGA GCAAGCTGCATCATTT-3′,gata4:F5′-CTGTCATCTCACTA TGGGCA — 3′,R,5′-CCAAGTCCGAGCAGGAATTT — 3′,NK 2homeobox5(nkx2-5):F5′-AAGCAACAGCGGTACCTGTC-3′, R,5′-GCTGTCGCTTGCACTTGTAG — 3′,myosinheavychain7 (myh7):F5′-TTGGCACGGACTGCGTCATC — 3′,R,5′-GAGC CTCCAGAGTTTGCTGAAGGA — 3′,glyceraldehyde-3-phosp hatedehydrogenase(gapdh):F5′-CAGAAGACTGTGGATGGC CC-3′,R5′-AGTGTAGC- CCAGGATGCCCT-3′.

Immunofluorescence staining

Staining was performed as described (24). Primary antibodies: anti-tropomyosin (1:200, Sigma), anti-actinin (1:100, Abcam), anti-aurora B (1:200) (both BD Transduction Laboratories), rabbit polyclonal anti-troponin I, anti-cyclin A, anti-cyclin dependent kinase 1 (cdc2), anti-geminin (all 1:50, Santa Cruz Biotechnology), anti-phospho-histone H3 (Ser10) (1:200, Millipore), anti-pRb807/811 (1:100, Cell Signaling), anti-mAG (1:300, MBL), rat monoclonal anti-5-Bromo-2-deoxyuridine (BrdU) (1:100, Abcam). Immune complexes were detected with ALEXA 488- or ALEXA 594-conjugated secondary antibodies (1:200; Molecular Probes). DNA was visualized with DAPI'(4" 6'-diamidino-2-phenylindole, $0.5\,\mu g/ml$). For BrdU, cells were cultured in $30\,\mu M$ BrdU (Sigma) (neonatal: last 24–48 h, adult: last 5 days).

Culture and cardiac differentiation of human induced pluripotent stem cells (HiPSC)

The line hiPSC 19-9-11 (WISC Bank) was utilized to generate cardiomyocytes based on a previously published protocol (25). In brief, hiPSCs were maintained in mTeSR1 media (STEMCELL Technologies). When hiPSCs reached the proper confluency (∼80%), they were passaged using trypsin-EDTA (Life Technologies) and plated at a density of 200,000 cells per well of a Matrigel (BD Biosciences)-coated 24-well plates containing mTeSR with $10\,\mu M$ Rock Inhibitor (Y27632). After 24 h, media was changed with 0.5 mL mTeSR media without Rock inhibitor. At the following day, culture media was replaced with 50 nM XV (GSK3 inhibitor) in mTeSR media for hiPSC differentiation (Day 0). After 24 h, media was substituted with RPMI/B-27 minus insulin (Day 1). On Day 3, 50% of media was exchanged with RPMI/B-27 minus insulin and IWP-2 [Wnt signaling inhibitor, $7.5\,\mu M$ (final concentration)]. On day 5, media was replenished with RPMI/B27 minus insulin. On day 7, media was changed with RPMI/B27. Then, media was renewed every 3 days (we kept the cells for 36 days). Next, cells were trypsinized with 0.25% (wt/vol) trypsin-EDTA and incubated the mixture in a 37°C, 5% CO_2 incubator for 5 min. The cells were centrifuged at 200 x g for 5 min and the cell pellet was distributed in RPMI20 + $5\,\mu M$ Y27632 on a laminin-coated coverslip (25 μg/mL). After 2 days, the cells were kept in RPMI/B-27 medium and maintained for the desired time (for 2 days). HiPSC-derived cardiomyocytes were then stimulated with small molecules to analyze their effect on cell cycle progression.

MTS assay

Cell cytotoxicity was measured by an MTS assay (Abcam) according to the manufacture's instruction. Cardiomyocytes were treated with DMSO or individual small molecules for 72 h and absorbance was measured after MTS reagent addition at 4–0 - 500 nm using an Epoch microplate spectrophotometer (Biotek, USA).

Cell count

In order to determine whether compounds increase the number of cells, 100,000 neonatal rat cardiomyocytes were seeded per well of 24-well plates. Cells were then cultured for 48 h in the presence of $20\,\mu M$ ara C and 5% horse serum and subsequently treated with the indicated compounds in the presence of 0.2% FBS as indicated. The number of cells was determined 5 days post-treatment after trypsinization utilizing a TC20 cell counter (Bio-Rad, USA) according to the manufacturer's instructions.

Statistical analysis

For immunofluorescence analyses, around 50 cardiomyocytes in five random fields of two different subpopulations were counted per experiment equaling a total cell number of around 500 cardiomyocytes. Data of at least three independent experiments are expressed as mean ± standard error of the mean (SEM). Results were analyzed by Graph Pad Prism (version 4.00, Graph Pad Software Inc.). Statistical significance was determined using a two-tailed Student's t-test or analysis of variance (ANOVA) were appropriate. The values of $p < 0.05$ were considered statistically significant.

Results

Live cell screening based on mouse stem cell-derived cardiomyocytes

In order to perform a screen for novel inducers of cardiomyocyte cell cycle activity, we have generated a mouse stem cell line that expresses a non-functional human geminin deletion mutant fused to a monomeric version of AG [mAG-hGem(1/110)] under the control of the ubiquitous CMV promoter (Figure 1A). Note, mAG-hGem(1/110) is only stable in S-/G2-/ and M-phase cells. In order to develop this cell line, we transfected the mouse ES cell line CM7/1 (26) with the plasmid mAG-hGem(1/110) (18), which allows selection for positive integration with Zeocin. The cell line CM7/1 expresses the neomycin-phospho-transferase gene under the control of the cardiomyocyte-specific *α-myosin heavy chain* promoter. This allows to obtain stem cell-derived cardiomyocyte cultures with a purity of > 99% after G418-treatment (26). This approach resulted in the establishment of the cell line CM7/1-hgem expressing AG (Figure 1B), which can be induced to differentiate into well beating EBs (Figures 1C,D). To ensure that cardiomyocytes derived from CM7/1-hgem express mAG-hGem(1/110), 12–14 days-old beating EBs were dissociated and seeded cells were stained for AG and a cardiomyocyte-specific marker (Figure 1E). This analysis revealed that $22.3 \pm 6.8\%$ of cardiomyocytes expressed mAG-hGem(1/110). That mAG-hGem(1/110) expression does not interfere with cardiogenesis of CM7/1-hgem was validated by normal temporal mRNA expression patterns of stem cell (*oct3/4*, *nanog*), mesodermal (*brachyury*), early progenitor (*gata4*), and cardiomyocyte (*myh7*) markers (Figure 1F). The actual screen for novel inducers of cardiomyocyte cell cycle activity was performed with cardiomyocytes obtained by treating CM7/1-hgem EBs at day 9 of differentiation with G418, dissociation of these EBs at day 12 to 14, plating the single cells on fibronectin-coated plates, and culturing them for another 6 days in the presence of G418. Immunofluorescence analysis revealed that the percentage of non-myocytes in the single cell culture decreased from $68.6 \pm 5.8\%$ at day 1 to $<3.5 \pm 0.4\%$ at day 6 (mean $\pm$ SEM, ***: $p < 0.001$, Figures 1G,H).
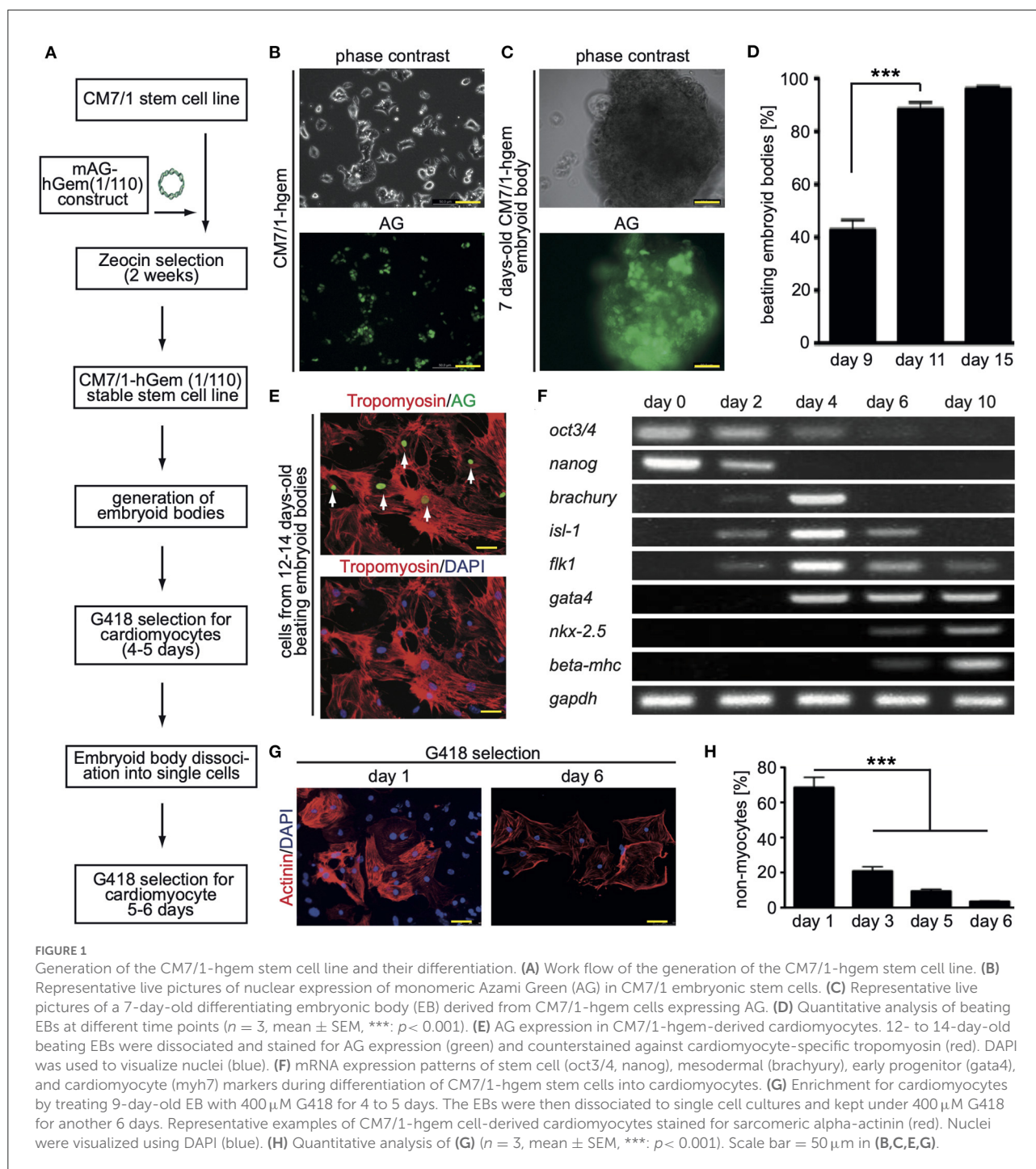
To assess the base level of CM7/1-hgem-derived cardiomyocyte cell cycle activity, BrdU incorporation (24 h) assays were performed and the number of mAG-hGem(1/110)-, H3P (histone H3 phosphorylation on serine 10)-positive as well as Aurora B-positive cardiomyocytes was determined at day 1 (non-selected) and day 6 (selected) post-dissociation. The number of cardiomyocytes incorporating BrdU decreased from $38.8 \pm 3.5\%$ at day 1 to $4.8 \pm 0.92\%$ at day 6 (mean $\pm$ SEM, $p < 0.01$, Figures 2A,B). Assuming that completion of one cell cycle lasts less than 24 hours, all cycling cardiomyocytes should be BrdU-positive. The percentage of cardiomyocytes expressing mAG-hGem(1/110) decreased from $22.3 \pm 3\%$ to $3 \pm 0.6\%$

(mean $\pm$ SEM, $p < 0.01$, Figures 2B,C). The overall number of mAG-hGem(1/110)-positive cells is as expected lower than BrdU-positive cells, as mAG-hGem(1/110) is only stable in S-/G2-/ and M-phase cells. The number of H3P-positive cardiomyocytes decreased from $5.9 \pm 0.45\%$ to $0.45 \pm 0.1\%$ (Figure 2D). Note, histone H3 is only phosphorylated in late G2-phase cells and M-phase cells until late anaphase. Finally, the number of Aurora B-positive cardiomyocytes at the midbody decreased from $1.89 \pm 0.1\%$ to $0.25 \pm 0.03\%$ (Figures 2E,F). Note, Aurora B is only a marker for cytokinesis when localized to the midbody or cleavage furrow. The overall decrease of cycling cardiomyocytes from day 1 to day 6 is in agreement with the general observation that the proliferation rate of ES cell-derived cardiomyocytes decreases over time in culture (27).

In order to test whether cell cycle activity in CM7/1-hgem-derived cardiomyocytes can be promoted, cells were stimulated for 3 days with 10% FBS, which is known to promote cell cycle activity in fetal, neonatal, and adult mammalian cardiomyocytes (24, 28). FBS treatment induced in $37 \pm 3.8\%$ of cardiomyocytes BrdU incorporation (Figures 2G,H), in $21 \pm 4.4\%$ mAG-hGem(1/110) expression (Figures 2H,I), and in $6 \pm 0.8\%$ histone H3 phosphorylation (Figures 2J,K) compared to $4.8 \pm 0.9\%$ (BrdU), $3 \pm 0.6\%$ (AG), and $0.49 \pm 0.09\%$ (H3P) upon DMSO treatment, respectively (mean $\pm$ SEM, $p < 0.01$, Figures 2H,K).

Screening for small molecules inducing CM7/1-hgem-derived cardiomyocyte cell cycle activity

In order to identify novel inducers of cardiomyocyte cell cycle activity, a subset of compounds of the small molecule library "Spectrum Collection" from MicroSource Discovery Systems, Inc. (Gaylordsville, CT) was utilized. This library presents 2,560 compounds and includes drugs from three sources: (1) US drug collection of 1,040 drugs that have reached clinical trial stages in the USA whereby each compound has been assigned USAN or USP status. (2) An International Drug Collection of 240 drugs that are marketed in Europe and/or Asia. (3) The rest is a unique collection of pure natural products and their derivatives. Natural Products include simple and complex oxygen heterocycles, alkaloids, sesquiterpenes, diterpenes, pentacyclic triterpenes, sterols, and many other diverse representatives. For each compound, data can be obtained regarding its structure, CAS #, formula, molecular weight, biological profile, as well as generic and market name. In addition, literature references are available describing the use and toxicology of the individual compounds. CM7/1-hgem-derived EB's were dissociated on day 14, seeded at 15,000 cells per well in a 96-well plate (flat glass-bottomed), and cultured for 6 days in the presence of G418. Subsequently, cells were treated with a subset of compounds of the small molecule

FIGURE 1

Generation of the CM7/1-hgem stem cell line and their differentiation. **(A)** Work flow of the generation of the CM7/1-hgem stem cell line. **(B)** Representative live pictures of nuclear expression of monomeric Azami Green (AG) in CM7/1 embryonic stem cells. **(C)** Representative live pictures of a 7-day-old differentiating embryonic body (EB) derived from CM7/1-hgem cells expressing AG. **(D)** Quantitative analysis of beating EBs at different time points ($n = 3$, mean ± SEM, ***: $p < 0.001$). **(E)** AG expression in CM7/1-hgem-derived cardiomyocytes. 12- to 14-day-old beating EBs were dissociated and stained for AG expression (green) and counterstained against cardiomyocyte-specific tropomyosin (red). DAPI was used to visualize nuclei (blue). **(F)** mRNA expression patterns of stem cell (oct3/4, nanog), mesodermal (brachyury), early progenitor (gata4), and cardiomyocyte (myh7) markers during differentiation of CM7/1-hgem stem cells into cardiomyocytes. **(G)** Enrichment for cardiomyocytes by treating 9-day-old EB with $400\,\mu M$ G418 for 4 to 5 days. The EBs were then dissociated to single cell cultures and kept under $400\,\mu M$ G418 for another 6 days. Representative examples of CM7/1-hgem cell-derived cardiomyocytes stained for sarcomeric alpha-actinin (red). Nuclei were visualized using DAPI (blue). **(H)** Quantitative analysis of **(G)** ($n = 3$, mean ± SEM, ***: $p < 0.001$). Scale bar = $50\,\mu m$ in **(B,C,E,G)**.

library "Spectrum Collection" at a concentration of $1\,\mu M$. DMSO served as a negative control, 10% FBS and FGF1/p38i as positive controls. mAG-hGem(1/110)-positive cells per field were recorded for 4 days at intervals of 12 h (Figure 3A). As this was a pilot study, recording (image acquisition) and image analysis were performed manually, and the screen was performed only once. Note, to minimize the manual

labor, only around 100 cells in the center of each well were evaluated utilizing a 20x objective. Data are represented as a fold-change increase of the observed maximal number of mAG-hGem(1/110)-positive cells per field in comparison to the maximal number in DMSO-treated cultures (Figure 3B). Note, in cases when compound treatment resulted in no mAG-hGem(1/110)-positive cell at markedly more time points
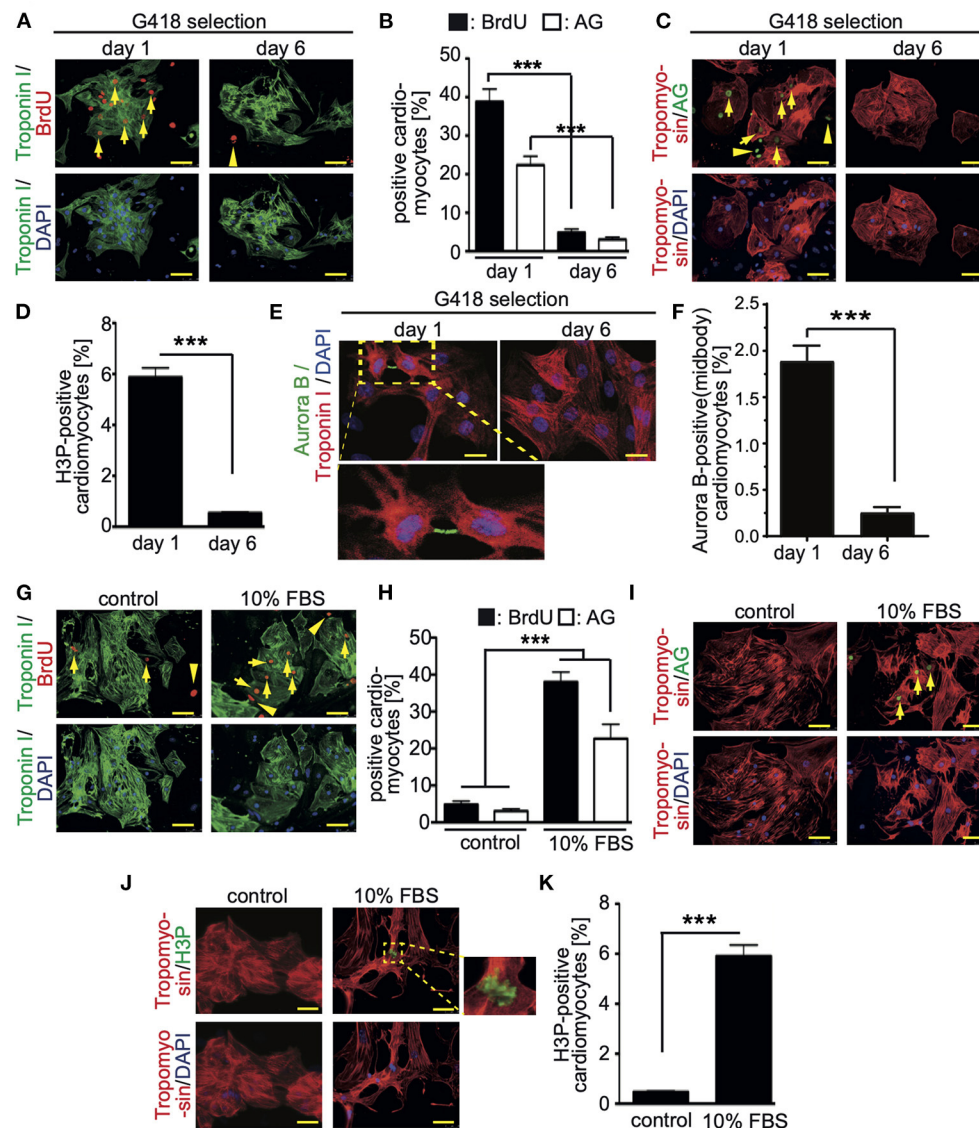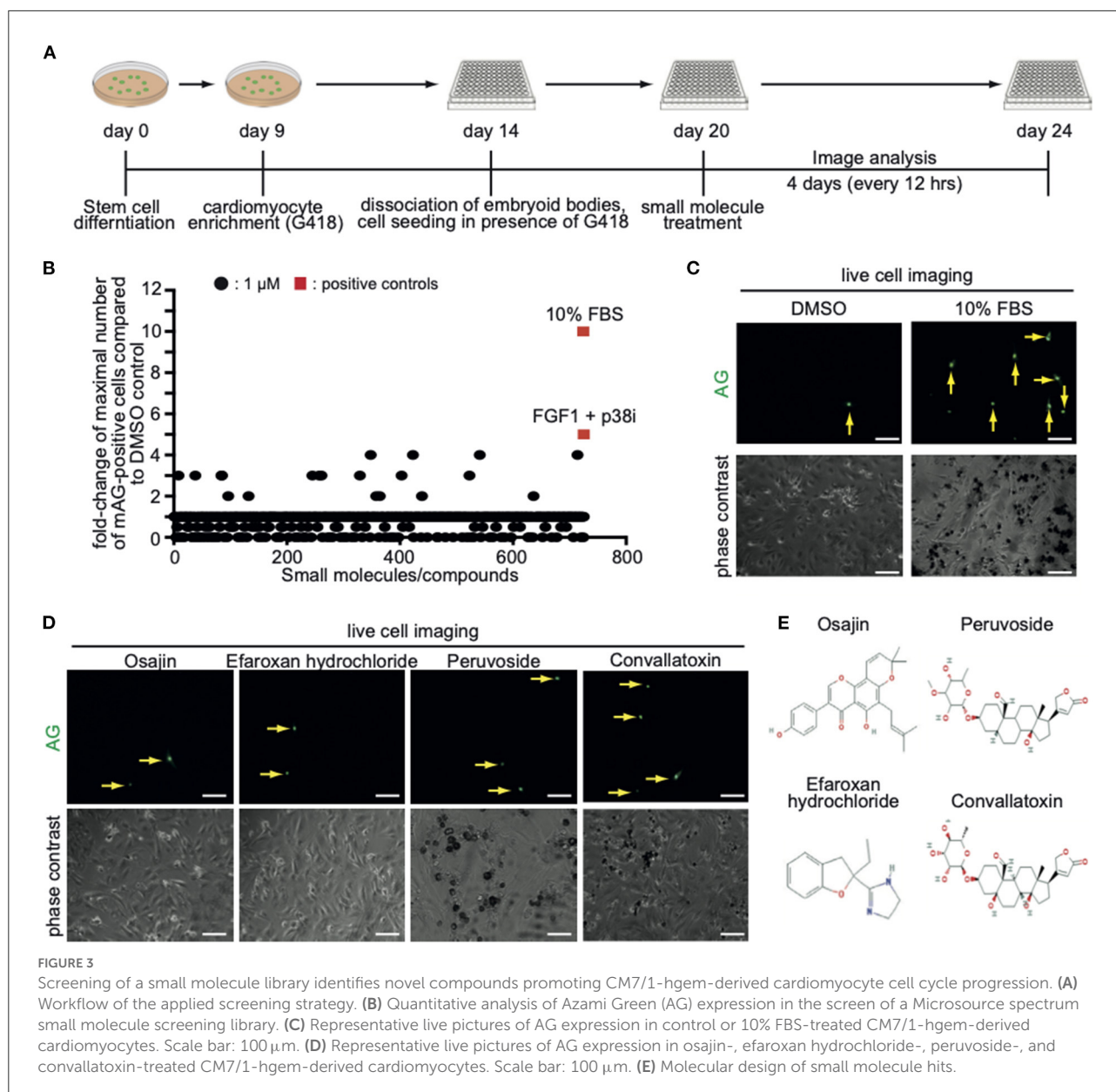
FIGURE 2

Cell cycle activity in CM7/1-hgem derived cardiomyocytes. **(A,C)** The number of BrdU- and Azami Green (AG)-positive CM7/1-hgem-derived cardiomyocytes decreased during differentiation. Representative examples of CM7/1-hgem-derived cardiomyocytes stained for troponin I (green) or tropomyosin (red) (cardiomyocyte-specific), BrdU (red) **(A)** or AG (green) **(C)**, and DAPI (nuclei, blue). Scale bar: 50 μm. $n = 6$. **(B)** Quantitative analysis of **(A,C)** ($n = 6$, mean ± SEM, ***:$p < 0.001$). **(D)** Quantitative analysis of H3P-positive CM7/1-hgem-derived cardiomyocytes ($n = 6$, mean ± SEM, ***:$p < 0.001$). **(E)** Representative examples of CM7/1-hgem-derived cardiomyocytes stained for troponin I (red) (cardiomyocyte-specific), Aurora B (green), and DAPI (nuclei, blue). Scale bar: 20 μm. **(F)** Quantitative analysis of Aurora B-positive CM7/1-hgem-derived cardiomyocytes at the midbody ($n = 6$, mean ± SEM, ***:$p < 0.001$). **(G–I)** Stimulation of cell cycle progression in CM7/1-hgem-derived cardiomyocytes by 10% FBS. Representative examples of CM7/1-hgem-derived cardiomyocytes stained for troponin I (green) **(G)** or tropomyosin (red) **(I)** (cardiomyocyte-specific), BrdU (red) **(G)** or AG (green) **(I)**, and DAPI (nuclei, blue). Scale bar: 50 μm. $n = 3$. **(F)** Quantitative analysis of **(G,I)** ($n = 6$, mean ± SEM, ***:$p < 0.001$). **(J)** Representative examples of CM7/1-hgem-derived cardiomyocytes stained for tropomyosin (red) (cardiomyocyte-specific), H3P (green), and DAPI (nuclei, blue). Scale bar: 50 μm. $n = 6$. **(K)** Quantitative analysis of **(J)** ($n = 6$, mean ± SEM, ***: $p < 0.001$).

($\geq$ 4) than in the DMSO control (1 of 8), the fold-change was defined as 0.5-fold. The number of observed mAG-hGem(1/110)-positive cells at the different 12 h time points for each treatment are provided in Supplementary Table 1. Our analysis revealed that 10% FBS as well as FGF1/p38i efficiently induced mAG-hGem(1/110) expression in CM7/1-hgem-derived cells enriched for cardiomyocytes (~10 fold and ~5-fold, respectively, Figures 3B,C). While most of the 722 tested compounds had no positive effect on mAG-hGem(1/110) expression, 19 compounds induced mAG-hGem(1/110)

FIGURE 3
Screening of a small molecule library identifies novel compounds promoting CM7/1-hgem-derived cardiomyocyte cell cycle progression. **(A)** Workflow of the applied screening strategy. **(B)** Quantitative analysis of Azami Green (AG) expression in the screen of a Microsource spectrum small molecule screening library. **(C)** Representative live pictures of AG expression in control or 10% FBS-treated CM7/1-hgem-derived cardiomyocytes. Scale bar: 100 μm. **(D)** Representative live pictures of AG expression in osajin-, efaroxan hydrochloride-, peruvoside-, and convallatoxin-treated CM7/1-hgem-derived cardiomyocytes. Scale bar: 100 μm. **(E)** Molecular design of small molecule hits.

expression in at least twice as many cells as upon DMSO treatment (Figure 3B, Supplementary Table 1). The most effective compounds were osajin, efaroxan hydrochloride, peruvoside, and convallatoxin (all 4-fold) (Figures 3D,E).

Cell cycle-promoting effect of identified compounds on neonatal and adult primary rat cardiomyocytes

Stem cell-derived cardiomyocytes are considered immature exhibiting a behavior similar to late fetal cardiomyocytes (29).

In order to assess whether the here identified 19 compounds could promote cell cycle progression also in more mature cardiomyocytes, neonatal rat cardiomyocytes were stimulated and analyzed 3 days later for BrdU incorporation (BrdU pulse-labeled for the final 24 h). For this purpose, cardiomyocytes were isolated from postnatal day 3 (P3) rats and stimulated once with the individual small molecules at concentrations of 50 nM, 250 nM, 1 μM, and 5 μM (Supplementary Figure 1).

Subsequently, cardiomyocytes were treated with the optimal concentrations of the individual compounds, cultured for 3 days and pulse-labeled with BrdU for the final 48 hours to assess also cardiomyocytes that already entered S phase after 24 h to 48 h post-treatment. In Supplementary Figure 1 (data from
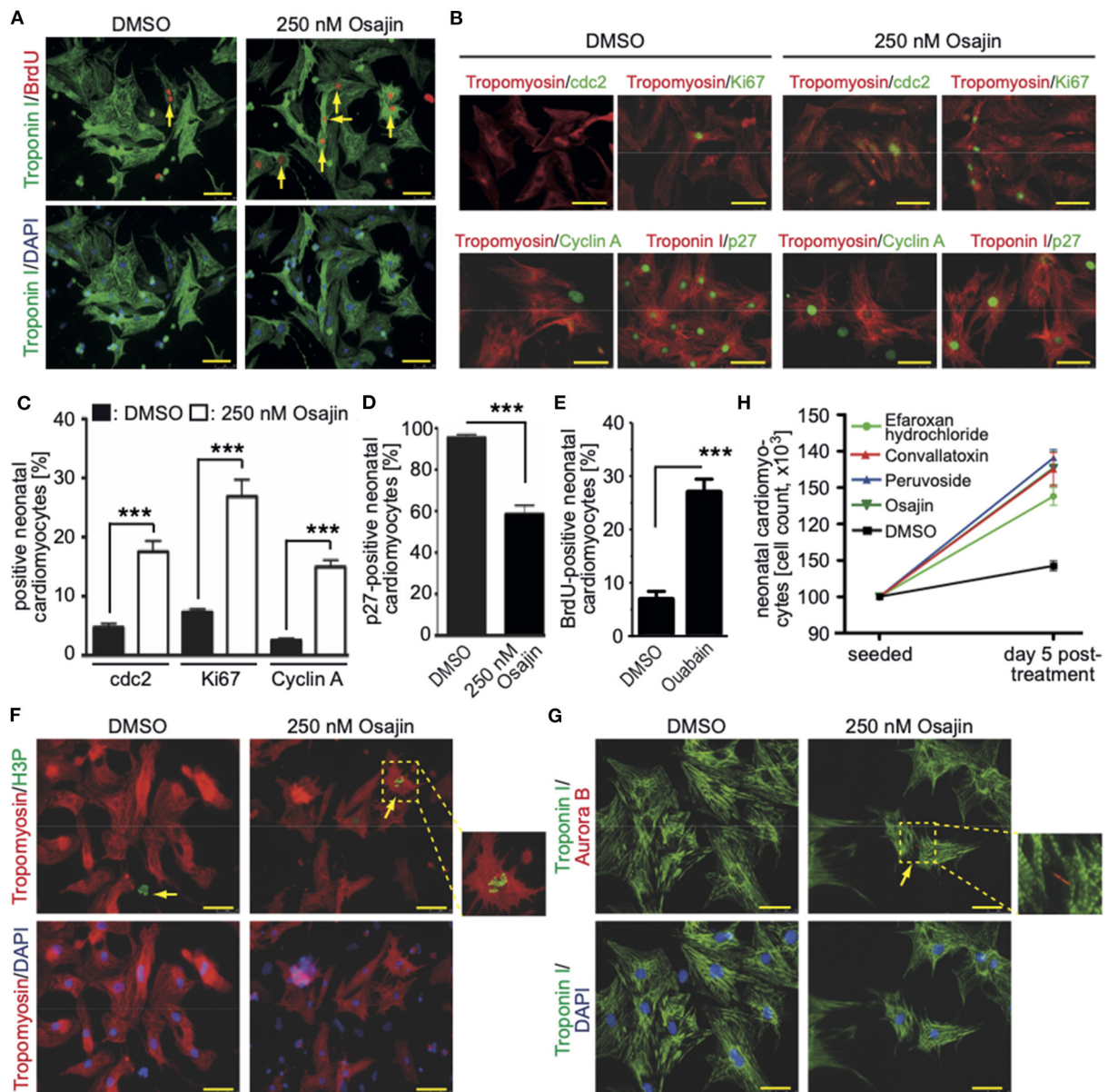
FIGURE 4
Promoting neonatal cardiomyocyte cell cycle progression by small molecules (Positive hits). **(A)** Osajin induced BrdU incorporation of P3 neonatal cardiomyocytes ($n = 6$). Representative example of neonatal cardiomyocytes stained for BrdU (red) and troponin I (green, cardiomyocyte-specific). Examples are indicated by arrows. DNA was visualized using DAPI (blue). **(B)** Osajin treatment induced increased expression of cell cycle promoting factors and decreased expression of cell cycle inhibitors (immunofluorescence analyses at 48 h after stimulation). Representative example of neonatal cardiomyocytes stained for cdc2, Ki67, cyclin A, or p27 (green) and tropomyosin (red, cardiomyocyte-specific). DNA was visualized using DAPI (blue). **(C,D)** Quantitative analysis of **(B)** ($n = 6$, mean ± SEM, ***: $p < 0.001$). **(E)** Quantitative analysis of the number of BrdU-positive cardiomyocytes after ouabain treatment ($n = 6$, mean ± SEM, ***: $p < 0.001$). **(F,G)** Representative examples of osajin-stimulated neonatal cardiomyocytes stained for tropomyosin (red) or troponin I (green, both cardiomyocyte-specific) undergoing mitosis (H3P, green) and cytokinesis (Aurora B, red). Examples are indicated by arrows. Arrowhead: H3P-positive non-myocyte. DNA was visualized using DAPI (blue). **(H)** Quantitative analysis of the increase in cell number five days after treatment with the indicated compounds ($n = 5$, mean ± SD). Scale bars: 50 μm.

six independent experiments per parameter) the data for the optimal concentration of each of the 19 compounds is provided whereby treatment with 250 nM osajin was most efficient in inducing BrdU incorporation in P3 rat cardiomyocytes (30.3 ± 2.4% *vs.* DMSO: 10.5 ± 0.9%, $p < 0.01$, Figure 4A). A deeper analysis showed that osajin treatment induced the expression of cell cycle perpetuating factors like cdc2, cyclin A, and Ki67 (Figures 4B,C) and the downregulation of the

TABLE 1 Cell cycle parameters in neonatal rat cardiomyocytes treated with selected small molecules.

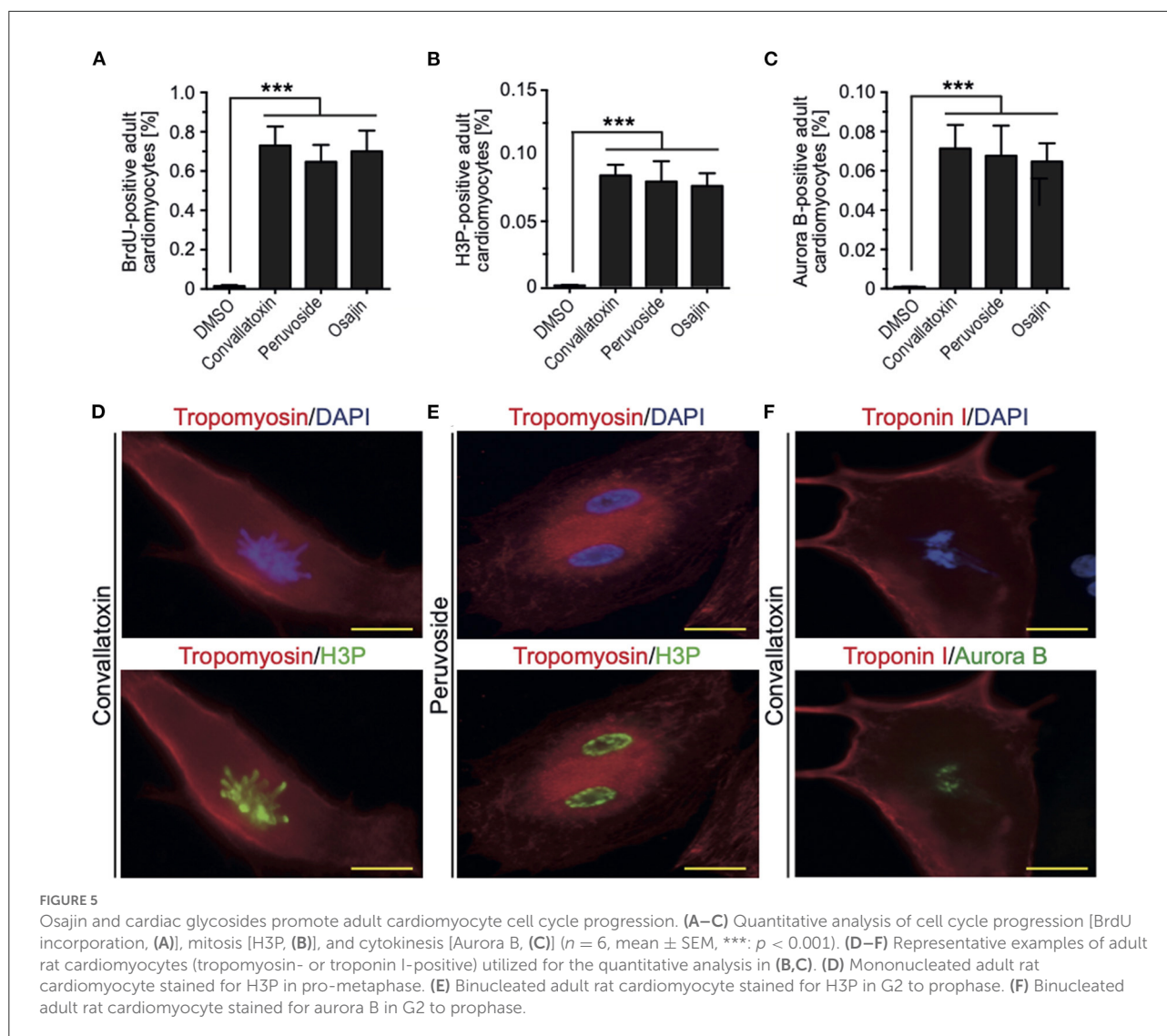| Small molecule	conc.	48 h BrdU [%]	H3P [%]	aurora B [%]
Osajin	0.25 µM	30.3 ± 2.4	1.86 ± 0.3	1.73 ± 0.3
Efaroxan Hydrochloride	1 µM	29.6 ± 2.1	1.76 ± 0.3	1.65 ± 0.3
Peruvoside	1 µM	30.0 ± 2.6	1.32 ± 0.2	1.36 ± 0.2
Convallatoxin	1 µM	29.3 ± 3.0	1.35 ± 0.3	1.28 ± 0.2
Valeryl salycilate	0.25 µM	27.0 ± 2.5	1.35 ± 0.1	1.21 ± 0.1
Idebenone	1 µM	22.0 ± 2.6	0.97 ± 0.1	0.92 ± 0.2
Lobaric acid	5 µM	22.0 ± 1.5	0.92 ± 0.2	0.85 ± 0.2
PIDOTIMOD	1 µM	21.3 ± 2.0	0.85 ± 0.1	0.75 ± 0.1
Ferulic acid	1 µM	22.6 ± 2.0	0.80 ± 0.2	0.75 ± 0.2
Quircitrin	1 µM	22.6 ± 0.8	0.75 ± 0.2	0.75 ± 0.1
Glutathione	1 µM	24.6 ± 2.3	0.60 ± 0.2	0.65 ± 0.2
Acedoben	1 µM	20.0 ± 3.2	0.65 ± 0.1	0.61 ± 0.1
Isaxonine	1 µM	21.6 ± 2.4	0.60 ± 0.2	0.50 ± 0.1
Protoporphyrin	1 µM	16.6 ± 3.8	0.55 ± 0.1	0.50 ± 0.1
N-methylanthranilic acid	1 µM	17.3 ± 1.8	0.60 ± 0.1	0.50 ± 0.1
Gitoxin	1 µM	19.0 ± 2.1	0.60 ± 0.1	0.50 ± 0.1
Tiratricol	1 µM	25.3 ± 3.7	0.55 ± 0.1	0.47 ± 0.1
Bilirubin	1 µM	18.6 ± 1.9	0.56 ± 0.2	0.45 ± 0.1
Merogedunin	1 µM	19.0 ± 1.2	0.35 ± 0.1	0.30 ± 0.1
DMSO		10.5 ± 0.9	0.37 ± 0.1	0.35 ± 0.1

cell cycle inhibitor p27 (Figures 4B,D). Notably, also the cardiac glycosides convallotoxin and peruvoside, efficiently induced BrdU incorporation (Supplementary Figure 1). Thus, we also tested the effect of the cardiac glycoside ouabain on P3 cardiomyocyte proliferation. Similar to the other cardiac glycosides, ouabain induced efficiently BrdU incorporation (28.8 ± 2.9% vs. DMSO: 9.1 ± 0.7%, $p < 0.01$, Figure 4E). Analyses of H3P revealed that all tested cardiac glycosides and all other compounds stimulating BrdU incorporation, except merogedunin, also induced cell cycle progression into G2/M-phase (Table 1). For example, treatment with 250 nM osajin induced the number of H3P-positive cardiomyocytes ∼5-fold compared to DMSO (1.86 ± 0.3% vs. DMSO: 0.37 ± 0.1%, $p < 0.01$) after 3 days of stimulation (Figure 4F). The analysis of aurora B expression suggests that most compounds, including osajin (1.73 ± 0.3%), efaroxan hydrochloride (1.65 ± 0.3%) as well as the cardiac glycosides peruvoside (1.36 ± 0.2%) and convallotoxin (1.28 ± 0.2% vs. DMSO: 0.35 ± 0.1%, $p < 0.01$), also induce cytokinesis (Table 1). Notably, cardiomyocytes exhibited in most cases a two-sided cleavage furrow, as shown for osajin (Figure 4G). Finally, cell count experiments revealed that the treatment of all compounds resulted 5 days post-treatment in a significantly increased cell number (Figure 4H). Notably, none of these compounds exhibited cytotoxic effects on cardiomyocytes based on MTS assays (Supplementary Figure 2). Taken together, our data suggest that our screening system allows the identification of

molecules with the potential to promote neonatal cardiomyocyte proliferation such as cardiac glycosides.

To determine if cardiac glycosides can also promote cell cycle progression in adult rat cardiomyocytes, ventricular cardiomyocytes from 12-week-old rats were stimulated and analyzed for BrdU incorporation, histone H3 phosphorylation, and aurora B expression. Osajin as well as the cardiac glycosides peruvoside and convallotoxin efficiently induced cell cycle re-entry in adult rat cardiomyocytes (all > 0.6% BrdU-, > 0.07% H3P-, and > 0.06% aurora B-positive cardiomyocytes compared to < 0.002% for all parameters upon DMSO treatment, Figures 5A–C). Notably, cell cycle activity was observed in mono- as well as binucleated adult rat cardiomyocytes (Figures 5D–F). Collectively, these data show that cardiac glycosides can promote adult cardiomyocyte cell cycle progression.

Identified compounds promote cell cycle progression of HiPSC-derived cardiomyocytes

Aiming at evaluating the translation potential of the identified compounds, the effect of the positive hits, including cardiac glycosides, on cell cycle progression in hiPSC-derived cardiomyocytes was assessed. HiPSC-derived cardiomyocytes were treated with DMSO or peruvoside (100 nM), convallotoxin
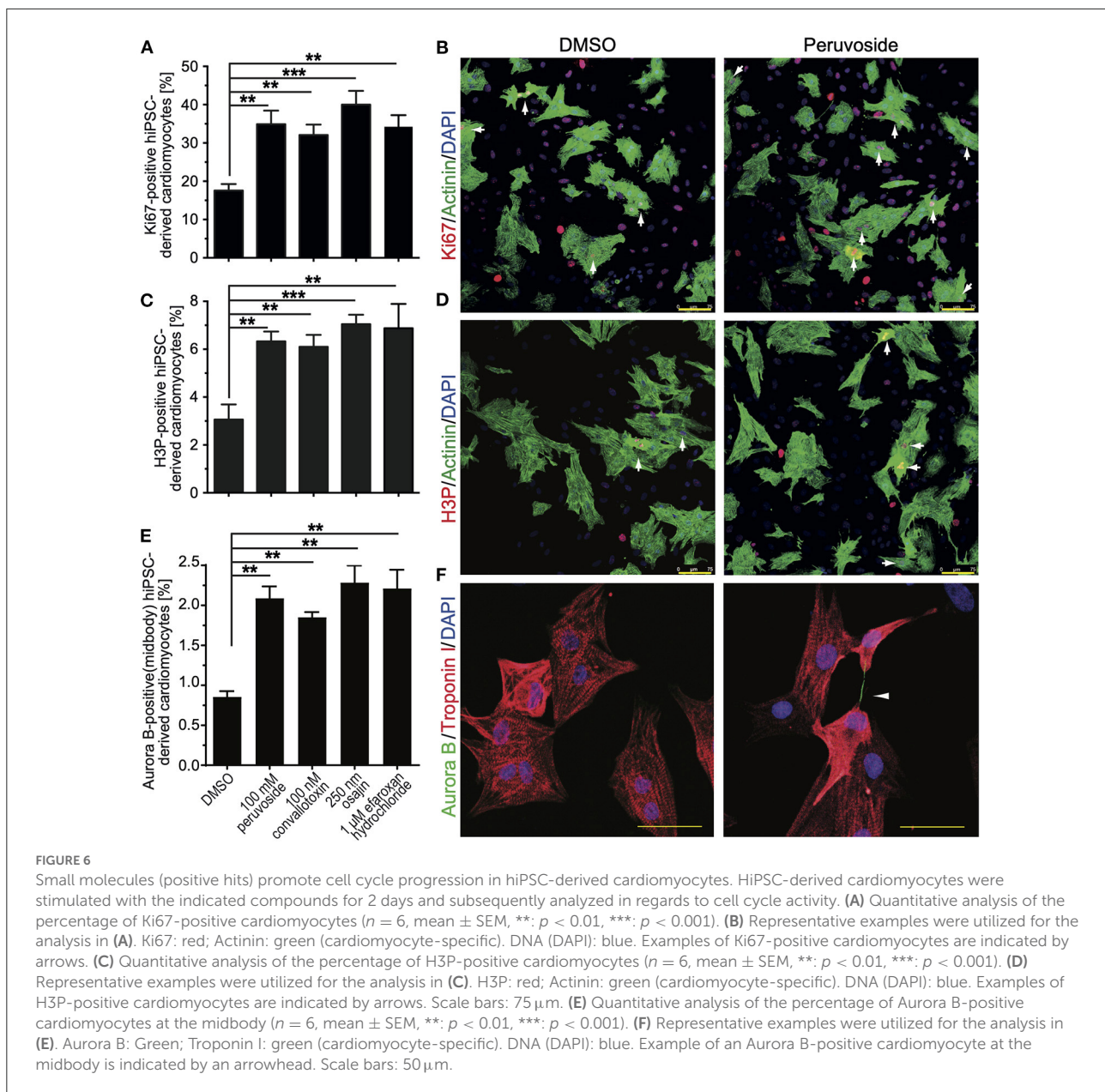
FIGURE 5
Osajin and cardiac glycosides promote adult cardiomyocyte cell cycle progression. **(A–C)** Quantitative analysis of cell cycle progression [BrdU incorporation, **(A)**], mitosis [H3P, **(B)**], and cytokinesis [Aurora B, **(C)**] ($n = 6$, mean ± SEM, ***: $p < 0.001$). **(D–F)** Representative examples of adult rat cardiomyocytes (tropomyosin- or troponin I-positive) utilized for the quantitative analysis in **(B,C)**. **(D)** Mononucleated adult rat cardiomyocyte stained for H3P in pro-metaphase. **(E)** Binucleated adult rat cardiomyocyte stained for H3P in G2 to prophase. **(F)** Binucleated adult rat cardiomyocyte stained for aurora B in G2 to prophase.

(100 nM), osajin (250 nM), and efaroxan hydrochloride (1 µM) and analyzed for changes in the expression of Ki67 or phosphorylation of histone H3 (H3P) 48 h post-treatment (Figures 6A–D). Pervuvoside significantly increased the number of both Ki67- and H3P-positive cardiomyocytes compared to DMSO (Ki67: 34.90 ± 2% *vs.* DMSO: 17.57 ± 0.97%, $p < 0.01$; H3P: 6.3 ± 0.23% *vs.* DMSO: 3.06 ± 0.36%, $p < 0.01$). Similarly, all other tested compounds exhibited a positive effect on cell cycle progression in hiPSC-derived cardiomyocytes (convallotoxin: Ki67: 32.07 ± 1.57%, H3P: 6.1 ± 0.28%; osajin: Ki67: 40.00 ± 2.0%, H3P: 7.04 ± 0.22%; efaroxan hydrochloride: Ki67: 34.25 ± 1.7%, H3P: 6.88 ± 0.58%; all $p < 0.01$, Figures 6A–D). Finally, we analyzed Aurora B-positive cardiomyocytes at midbody indicative for cell division. We found that pervuvoside significantly increased cardiomyocytes in cytokinesis compared to DMSO (Aurora B at midbody: 2.08 ± 0.08% *vs.* DMSO: 0.85 ± 0.04%, $p < 0.01$)

(Figures 6E,F). Similarly, all other tested compounds exhibited a positive effect on cardiomyocyte cytokinesis (convallotoxin: 1.85 ± 0.04%; osajin: 2.28 ± 0.12%; efaroxan hydrochloride: 2.21 ± 0.13%; all $p < 0.01$, Figure 6E). Taken together, these data suggest that cardiac glycosides, as well as osajin and efaroxan hydrochloride, also positively affect cell cycle progression in hiPSC-derived cardiomyocytes.
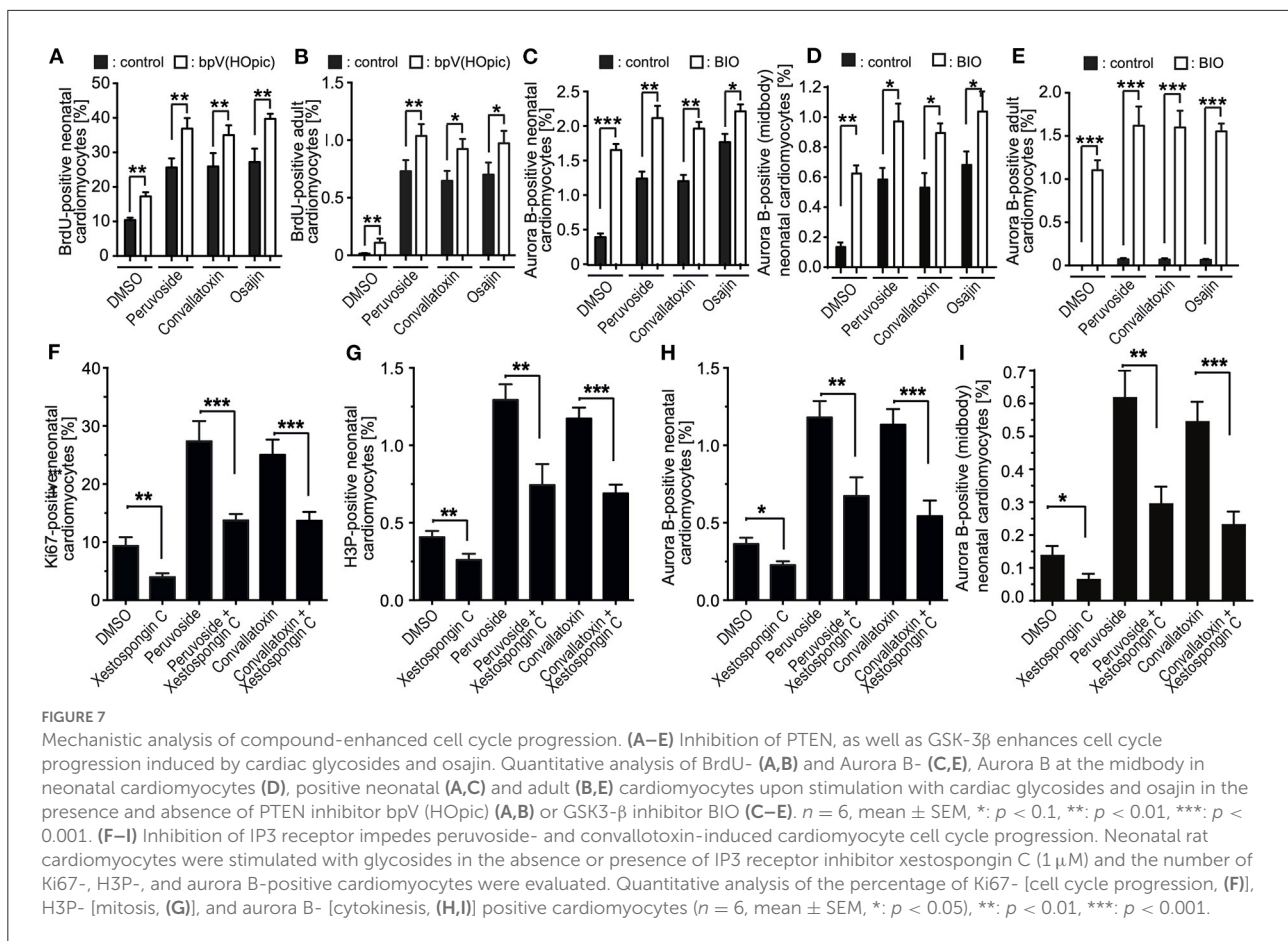
Inhibition of PTEN and GSK-3β enhance cell cycle progression induced by cardiac glycosides and osajin

Previously, others and we have shown that the phosphoinositide 3-kinase (PI3K)-Akt pathway is implicated in the regulation of cardiomyocyte proliferation (14, 24, 30)

FIGURE 6

Small molecules (positive hits) promote cell cycle progression in hiPSC-derived cardiomyocytes. HiPSC-derived cardiomyocytes were stimulated with the indicated compounds for 2 days and subsequently analyzed in regards to cell cycle activity. **(A)** Quantitative analysis of the percentage of Ki67-positive cardiomyocytes ($n = 6$, mean ± SEM, **: $p < 0.01$, ***: $p < 0.001$). **(B)** Representative examples were utilized for the analysis in **(A)**. Ki67: red; Actinin: green (cardiomyocyte-specific). DNA (DAPI): blue. Examples of Ki67-positive cardiomyocytes are indicated by arrows. **(C)** Quantitative analysis of the percentage of H3P-positive cardiomyocytes ($n = 6$, mean ± SEM, **: $p < 0.01$, ***: $p < 0.001$). **(D)** Representative examples were utilized for the analysis in **(C)**. H3P: red; Actinin: green (cardiomyocyte-specific). DNA (DAPI): blue. Examples of H3P-positive cardiomyocytes are indicated by arrows. Scale bars: 75 μm. **(E)** Quantitative analysis of the percentage of Aurora B-positive cardiomyocytes at the midbody ($n = 6$, mean ± SEM, **: $p < 0.01$, ***: $p < 0.001$). **(F)** Representative examples were utilized for the analysis in **(E)**. Aurora B: Green; Troponin I: green (cardiomyocyte-specific). DNA (DAPI): blue. Example of an Aurora B-positive cardiomyocyte at the midbody is indicated by an arrowhead. Scale bars: 50 μm.

and phosphatase and tensin homolog (PTEN), an inhibitor of the PI3K pathway, inhibits periostin-induced cardiomyocyte cell cycle activity (30). Recently, it was shown that loss of PTEN promotes cardiomyocyte proliferation and cardiac repair after MI, suggesting the pathway has a substantial role in cardiomyocyte proliferation (31). Thus, we have tested whether bpv(HOpic), a potent inhibitor of PTEN, enhances the effect of osajin and the cardiac glycosides on BrdU incorporation in neonatal and adult cardiomyocytes. As expected, bpv(HOpic) increased the number of BrdU-positive cardiomyocytes in the control, but was less efficient than osajin and the cardiac glucosides (Figures 7A,B). Notably, bpv(HOpic) significantly

enhanced the effect of osajin and the cardiac glucosides on inducing BrdU incorporation in primary neonatal (Figure 7A) as well as adult (Figure 7B) rat cardiomyocytes. In addition, we have previously demonstrated that the small molecule BIO, a specific inhibitor of glycogen synthase kinase-3 (GSK-3), promotes cell cycle progression into mitosis in neonatal and adult mammalian cardiomyocytes (14, 32). Thus, we have tested whether BIO enhances the effect of osajin and the cardiac glycosides in regards to aurora B expression in neonatal and adult cardiomyocytes (Figures 7C,E). While BIO had a moderate effect on aurora B expression in neonatal cardiomyocytes (Figure 7C) and aurora B-positive neonatal

FIGURE 7
Mechanistic analysis of compound-enhanced cell cycle progression. **(A−E)** Inhibition of PTEN, as well as GSK-3β enhances cell cycle progression induced by cardiac glycosides and osajin. Quantitative analysis of BrdU- **(A,B)** and Aurora B- **(C,E)**, Aurora B at the midbody in neonatal cardiomyocytes **(D)**, positive neonatal **(A,C)** and adult **(B,E)** cardiomyocytes upon stimulation with cardiac glycosides and osajin in the presence and absence of PTEN inhibitor bpV (HOpic) **(A,B)** or GSK-3-β inhibitor BIO **(C−E)**. $n = 6$, mean ± SEM, *: $p < 0.1$, **: $p < 0.01$, ***: $p < 0.001$. **(F−I)** Inhibition of IP3 receptor impedes peruvoside- and convallotoxin-induced cardiomyocyte cell cycle progression. Neonatal rat cardiomyocytes were stimulated with glycosides in the absence or presence of IP3 receptor inhibitor xestospongin C ($1 \mu M$) and the number of Ki67-, H3P-, and aurora B-positive cardiomyocytes were evaluated. Quantitative analysis of the percentage of Ki67- [cell cycle progression, **(F)**], H3P- [mitosis, **(G)**], and aurora B- [cytokinesis, **(H,I)**] positive cardiomyocytes ($n = 6$, mean ± SEM, *: $p < 0.05$), **: $p < 0.01$, ***: $p < 0.001$.

cardiomyocytes at the midbody (Figure 7D), it markedly enhanced aurora B expression in adult cardiomyocytes stimulated with osajin or the cardiac glycosides (Figure 7E). Yet, no adult cardiomyocytes positive for Aurora B at the midbody or cleavage furrow was observed. Yet, considering the rare observation of aurora B-positive adult cardiomyocytes and the short existence of the midbody, it is also rather unlikely to find an adult cardiomyocyte in this stage.

IP3 receptor inhibition reduces the cell cycle-promoting effect of cardiac glycosides

Cardiac glycosides increase the output force of the heart and decrease its rate of contractions by acting on the cellular sodium-potassium ATPase pump, Na$^+$K$^+$ATPase (20). As Na$^+$K$^+$ATPase is known to specifically regulate calcium transients *via* the inositol trisphosphate (IP3) receptors (33– 35), we have tested the effect of the selective IP3 receptor antagonist xestospongin C (36) on cardiac glycoside-enhanced cardiomyocyte cell cycle progression. For this purpose, P3

rat cardiomyocytes were stimulated with glycosides in the absence or presence of $1 \mu M$ xestospongin C and the number of Ki67-, H3P-, aurora B-positive cardiomyocytes as well as cardiomyocytes positive for aurora B at the midbody were evaluated. This analysis revealed that the presence of xestospongin C significantly reduced the positive effect of peruvoside and convallotoxin on neonatal cardiomyocyte cell cycle progression (Figures 7F–I). These data suggest that Ca2+ levels regulated by glycosides might be important for the cell cycle promoting effect of cardiac glycosides.

Discussion

Here we developed a fluorescence-based live imaging screening assay based on mouse stem cells and the Fucci system to identify new inducers of cardiomyocyte proliferation. This system eliminates the need for immunofluorescence staining, incorporation of nucleotide analogs or cell count assays and allows to capture events that may develop at different times post-treatment, which may be potentially overlooked by end-point assays. As the system utilizes a ubiquitous promoter, this system can also be utilized to identify new inducers of

proliferation of other cell types, such as neurons. Validation of positive hits utilizing several independent assays in primary neonatal and adult mammalian cardiomyocytes identified among others cardiac glycosides as a novel potential inducer of mammalian postnatal cardiomyocytes. In addition, the effect of cardiac glycosides on cardiomyocyte cell cycle progression was enhanced by inhibition of PTEN as well as GSK-3β and inhibited by IP3 receptor antagonist xestospongin C, which is known to inhibit IP3-mediated Ca^{2+} release from endo- and sarcoplasmic reticulum (36).

The here developed assay proved to be valid to identify novel compounds to enhance cardiomyocyte cell cycle progression. While our study is a pilot study being limited in a number of compounds, a number of analyzed cells per time point, and repetitions, pipette robots and automated image analysis solutions will allow in the future unbiased, in-depth analyses of high-content compound libraries.

To date, no direct data are available regarding the effect of cardiac glycoside on cardiomyocyte proliferation. In general, cardiac glycosides inhibit the sodium-potassium pump resulting in an increased calcium concentration inside the cell. It is well known that $Na^+K^+ATPase$ specifically regulates calcium transients *via* the IP3 receptors (33–35) and our data show that inhibition of the IP3 receptors with xestospongin C inhibits the cell cycle-promoting effect of glycosides. Notably, calcium plays, in general, a crucial role in cell proliferation and aberrant Ca^{2+}-signaling and loss of intracellular Ca^{2+} homeostasis contributes to tumor initiation and proliferation (37, 38). While cardiac glycosides became recently popular to inhibit tumor growth (39), there is evidence that cardiac glycosides can promote cell proliferation at lower, subsaturating concentrations. It has been reported that low concentrations of cardiac glycosides stimulate cell proliferation in astrocytes (40), vascular smooth muscle cells (41), renal tubule cells (42–44), Sertoli cells (45), human endothelial cells (46), and human umbilical vein smooth muscle cells (47). In addition, it has been indicated that voltage-gated L-type Ca^{2+} channels blockers enhance hiPSC-derived cardiomyocyte proliferation (48). Further, it has been reported that modulation of calcium channel activity controls proliferation vs. differentiation of cardiac progenitor cells (49). Finally, it has been suggested that cardiac glycosides can interfere with nuclear receptor signaling (19). For example, it has been shown that the cardiac glycosides digoxin and lanatoside C induce both the expression of peroxisome proliferator-activated receptor (PPAR) δ (50–52), which previously has been shown to promote cardiomyocyte proliferation (14). Taken together, our data indicate that cardiac glycosides can enhance cell cycle progression in cardiomyocytes.

Besides cardiac glycosides, we have identified the flavonoid osajin as a potent inducer of postnatal cardiomyocyte cell cycle progression. Previously, it has been shown that osajin exhibits a potential cardioprotective role in ischemia-reperfusion-induced injury in rat hearts. This cardioprotective role has been attributed to the suppression of oxidative stress resulting in improved ventricular function (53, 54). Yet, it has also been shown that osajin can inhibit fatty acid synthase (FASN) expression, a key enzyme for lipogenesis (55). This might enhance glycolysis, which has been associated with several processes during tissue repair and regeneration (56) as well as cardiomyocyte proliferation (13, 57). Concurrently, it has been shown that myocardial injury due to ischemia/reperfusion injury was significantly reduced by cardiac-specific PPARδ overexpression concomitant with increased myocardial glucose utilization (58).

Finally, we identified the selective α-adrenoceptor antagonist and imidazoline I_1 receptor ligand efaroxan hydrochloride as a promotor of cardiomyocyte cell cycle progression. α-adrenoceptor and imidazoline I_1 receptor are both expressed in cardiomyocytes and are involved in NO synthesis and intracellular calcium handling (59). Besides, efaroxan hydrochloride improved *in vivo* oral glucose tolerance (60). Yet, there is little evidence that efaroxan hydrochloride promotes proliferation. It has been reported that α2-adrenergic blockade by efaroxan hydrochloride increased primary breast tumor size and distant metastasis under non-stress conditions (61).

The efficiency of the investigated compounds to enhance cardiomyocyte cell cycle progression significantly decreased with the age of the cardiomyocytes. This phenomenon has been observed for a large number of measures to induce cardiomyocyte proliferation such as treatment with FGF1/p38 inhibitor, BIO or microRNAs as well as Meis1 deletion (24, 32, 62, 63). Thus, it will be important to elucidate the mechanisms promoting cardiomyocyte cell cycle progression utilized by the different stimuli, to determine the difference in the response of neonatal and adult cardiomyocytes to these stimuli, and to test if combinations of the different inhibitors might be able to induce robust proliferation in adult cardiomyocytes. Here, we have shown that the combinatorial approach of osajin or cardiac glycosides with PTEN or GSK3β inhibition enhances the effect on cardiomyocyte cell cycle progression. Similarly, it has been shown that the combinations of p38 MAP kinase inhibition/ PI3kinase/AKT signaling (24), GSK3β inhibition/AKT phosphorylation (4), and PPARδ signaling/GSK3β inhibition are more efficient in promoting cardiomyocyte cell cycle progression than the individual measures (14).

In the future, it will be important to determine whether the here identified drugs induce cell cycle re-entry of adult cardiomyocytes upon injury *in vivo* and to show that this contributes to improved function. Our data suggest that the positive effect of cardiac glycosides on heart function might not only increase myocardial contraction force by inhibiting the sodium-potassium pump but might also contribute to cardiac repair by inducing cardiomyocyte proliferation. Considering the toxicity of cardiac glycosides, the application of subsaturating

concentrations might open new avenues for the use of cardiac glycosides, which might benefit from the combination with other pro-proliferative drugs.

Conclusion

Considering that cardiovascular diseases represent a significant socio-economic burden affecting the pediatric as well as adult population and that currently no therapy is available to cure congenital heart disease or heart failure, the development of a cardiomyocyte proliferation screening system and the identification of novel inducers of cardiomyocyte proliferation, are potentially of great therapeutic value (64–66). Here, we identified, utilizing a novel screening system, potential compounds to promote cardiomyocyte proliferation including cardiac glycosides. Our data suggest that modulation of calcium handling and metabolism promotes cardiomyocyte proliferation and cardiac glycosides might, besides increasing myocardial contraction force, contribute to cardiac repair by inducing cardiomyocyte proliferation. The cardiomyocyte proliferation by cardiac glycosides at low concentrations enhanced by PTEN and GSK-3β inhibitors might contribute to cardiac repair by inducing cardiomyocyte proliferation. This study provides a translational perspective to investigate chemical compounds derived from the high throughput screening for their potential to improve cardiac tissue engineering approaches as well as to repair or regenerate the injured heart in pre-clinical models.

Data availability statement

The original contributions presented in the study are included in the article/Supplementary material, further inquiries can be directed to the corresponding authors.

Ethics statement

The animal study was reviewed and approved by the local Animal Ethics Committee Erlangen, Germany in accordance with governmental and international guidelines on animal experimentation (protocol TS-9/2016 Nephropatho).

Author contributions

AM designed and carried out most of the experiments, analyzed most of the data, and wrote the manuscript. HR performed *in vitro* cell culture and immunostaining. NS performed immunostainings. CE provided the human iPSC-derived differentiated cardiomyocytes. RK analyzed data and revised the manuscript. FE designed experiments, analyzed data, and wrote the manuscript. All authors contributed to the article and approved the submitted version.

Conflict of interest

The authors declare that the research was conducted in the absence of any commercial or financial relationships that could be construed as a potential conflict of interest.

Publisher's note

All claims expressed in this article are solely those of the authors and do not necessarily represent those of their affiliated organizations, or those of the publisher, the editors and the reviewers. Any product that may be evaluated in this article, or claim that may be made by its manufacturer, is not guaranteed or endorsed by the publisher.

Supplementary material

The Supplementary Material for this article can be found online at: https://www.frontiersin.org/articles/10.3389/fcvm.2022.901396/full#supplementary-material

SUPPLEMENTARY FIGURE 1
Dosage-dependent induction of DNA synthesis in neonatal cardiomyocytes. Quantitative analysis of BrdU-positive neonatal cardiomyocytes upon stimulation with the top 19 candidates at indicated concentrations. $n = 6$, mean $\pm$ SEM. Cardiomyocytes were isolated from postnatal day 3 rats, stimulated once with the individual small molecules, after 48 h BrdU was added, and after 24 h BrdU pulse-labeling the percentage of BrdU-positive cardiomyocytes was determined.

SUPPLEMENTARY FIGURE 2
Cardiac glycosides do not induce cell death in neonatal rat cardiomyocytes. Quantitative analysis of cardiomyocytes death by MTS assay ($n = 6$, mean $\pm$ SEM, **: $p < 0.01$, *: $p < 0.05$).

References

1. Virani SS, Alonso A, Benjamin EJ, Bittencourt MS, Callaway CW, Carson AP, et al. Heart Disease and Stroke Statistics-2020 Update: a report from the American Heart association. *Circulation.* (2020) 141:e139–596. doi: 10.1161/CIR.0000000000000757

2. Leone M, Engel FB. Advances in heart regeneration based on cardiomyocyte proliferation and regenerative potential of binucleated cardiomyocytes and polyploidization. *Clin Sci (Lond).* (2019) 133:1229–53. doi: 10.1042/CS20180560

3. Madonna R, Van Laake LW, Botker HE, Davidson SM, De Caterina R, Engel FB, et al. ESC Working Group on Cellular Biology of the Heart: position paper for Cardiovascular Research: tissue engineering strategies combined with cell therapies for cardiac repair in ischaemic heart disease and heart failure. *Cardiovasc Res.* (2019) 115:488–500. doi: 10.1093/cvr/cvz010

4. Buikema JW, Lee S, Goodyer WR, Maas RG, Chirikian O, Li G, et al. Wnt activation and reduced cell-cell contact synergistically induce massive expansion of functional human iPSC-derived cardiomyocytes. *Cell Stem Cell.* (2020) 27:50–63 e5. doi: 10.1016/j.stem.2020.06.001

5. Hesselbarth R, Esser TU, Roshanbinfar K, Schrufer S, Schubert DW, Engel FB. CHIR99021 promotes hiPSC-derived cardiomyocyte proliferation in engineered 3D microtissues. *Adv Healthc Mater.* (2021) 10:e2100926. doi: 10.1002/adhm.202100926

6. Bergmann O, Zdunek S, Felker A, Salehpour M, Alkass K, Bernard S, et al. Dynamics of cell generation and turnover in the human heart. *Cell.* (2015) 161:1566–75. doi: 10.1016/j.cell.2015.05.026

7. Becker JR, Deo RC, Werdich AA, Panakova D, Coy S, MacRae CA. Human cardiomyopathy mutations induce myocyte hyperplasia and activate hypertrophic pathways during cardiogenesis in zebrafish. *Dis Model Mech.* (2011) 4:400–10. doi: 10.1242/dmm.006148

8. Ben-Yair R, Butty VL, Busby M, Qiu Y, Levine SS, Goren A, et al. H3K27me3-mediated silencing of structural genes is required for zebrafish heart regeneration. *Development.* (2019) 146:dev178632. doi: 10.1242/dev.178632

9. Jiang J, Burgon PG, Wakimoto H, Onoue K, Gorham JM, O'Meara CC, et al. Cardiac myosin binding protein C regulates postnatal myocyte cytokinesis. *Proc Natl Acad Sci U S A.* (2015) 112:9046–51. doi: 10.1073/pnas.1511004112

10. Liu Z, Yue S, Chen X, Kubin T, Braun T. Regulation of cardiomyocyte polyploidy and multinucleation by CyclinG1. *Circ Res.* (2010) 106:1498–506. doi: 10.1161/CIRCRESAHA.109.211888

11. Sdek P, Zhao P, Wang Y, Huang CJ, Ko CY, Butler PC, et al. Rb and p130 control cell cycle gene silencing to maintain the postmitotic phenotype in cardiac myocytes. *J Cell Biol.* (2011) 194:407–23. doi: 10.1083/jcb.201012049

12. Zebrowski DC, Vergarajauregui S, Wu CC, Piatkowski T, Becker R, Leone M, et al. Developmental alterations in centrosome integrity contribute to the post-mitotic state of mammalian cardiomyocytes. *Elife.* (2015) 4. doi: 10.7554/eLife.05563

13. Cardoso AC, Lam NT, Savla JJ, Nakada Y, Pereira AHM, Elnwasany A, et al. Mitochondrial substrate utilization regulates cardiomyocyte cell cycle progression. *Nat Metab.* (2020) 2:167–78. doi: 10.1038/s42255-020-0169-x

14. Magadum A, Ding Y, He L, Kim T, Vasudevarao MD, Long Q, et al. Live cell screening platform identifies PPARdelta as a regulator of cardiomyocyte proliferation and cardiac repair. *Cell Res.* (2017) 27:1002–19. doi: 10.1038/cr.2017.84

15. Zebrowski DC, Becker R, Engel FB. Towards regenerating the mammalian heart: challenges in evaluating experimentally induced adult mammalian cardiomyocyte proliferation. *Am J Physiol Heart Circ Physiol.* (2016) 310:H1045–54. doi: 10.1152/ajpheart.00697.2015

16. Jung JH, Ikeda G, Tada Y, von Bornstadt D, Santoso MR, Wahlquist C, et al. miR-106a-363 cluster in extracellular vesicles promotes endogenous myocardial repair via Notch3 pathway in ischemic heart injury. *Basic Res Cardiol.* (2021) 116:19. doi: 10.1007/s00395-021-00858-8

17. Abbas N, Perbellini F, Thum T. Non-coding RNAs: emerging players in cardiomyocyte proliferation and cardiac regeneration. *Basic Res Cardiol.* (2020) 115:52. doi: 10.1007/s00395-020-0816-0

18. Sakaue-Sawano A, Kurokawa H, Morimura T, Hanyu A, Hama H, Osawa H, et al. Visualizing spatiotemporal dynamics of multicellular cell-cycle progression. *Cell.* (2008) 132:487–98. doi: 10.1016/j.cell.2007.12.033

19. Karas K, Salkowska A, Dastych J, Bachorz RA, Ratajewski M. Cardiac glycosides with target at direct and indirect interactions with nuclear receptors. *Biomed Pharmacother.* (2020) 127:110106. doi: 10.1016/j.biopha.2020.110106

20. Patel S. Plant-derived cardiac glycosides: Role in heart ailments and cancer management. *Biomed Pharmacother.* (2016) 84:1036–41. doi: 10.1016/j.biopha.2016.10.030

21. Muller-Ehmsen J, Nickel J, Zobel C, Hirsch I, Bolck B, Brixius K, et al. Longer term effects of ouabain on the contractility of rat isolated cardiomyocytes and on the expression of Ca and Na regulating proteins. *Basic Res Cardiol.* (2003) 98:90–6. doi: 10.1007/s00395-003-0396-9

22. Leone M, Engel FB. Isolation, culture, and live-cell imaging of primary rat cardiomyocytes. *Methods Mol Biol.* (2021) 2158:109–24. doi: 10.1007/978-1-0716-0668-1_9

23. Schroeder M, Niebruegge S, Werner A, Willbold E, Burg M, Ruediger M, et al. Differentiation and lineage selection of mouse embryonic stem cells in a stirred bench scale bioreactor with automated process control. *Biotechnol Bioeng.* (2005) 92:920–33. doi: 10.1002/bit.20668

24. Engel FB, Schebesta M, Duong MT, Lu G, Ren S, Madwed JB, et al. p38 MAP kinase inhibition enables proliferation of adult mammalian cardiomyocytes. *Genes Dev.* (2005) 19:1175–87. doi: 10.1101/gad.1306705

25. Lian X, Zhang J, Azarin SM, Zhu K, Hazeltine LB, Bao X, et al. Directed cardiomyocyte differentiation from human pluripotent stem cells by modulating Wnt/beta-catenin signaling under fully defined conditions. *Nat Protoc.* (2013) 8:162–75. doi: 10.1038/nprot.2012.150

26. Zweigerdt R, Burg M, Willbold E, Abts H, Ruediger M. Generation of confluent cardiomyocyte monolayers derived from embryonic stem cells in suspension: a cell source for new therapies and screening strategies. *Cytotherapy.* (2003) 5:399–413. doi: 10.1080/14653240310003062

27. Klug MG, Soonpaa MH, Field LJ, DNA. synthesis and multinucleation in embryonic stem cell-derived cardiomyocytes. *Am J Physiol.* (1995) 269:H1913–21. doi: 10.1152/ajpheart.1995.269.6.H1913

28. Engel FB, Schebesta M, Keating MT. Anillin localization defect in cardiomyocyte binucleation. *J Mol Cell Cardiol.* (2006) 41:601–12. doi: 10.1016/j.yjmcc.2006.06.012

29. Maxwell JT, Xu C. Stem-cell-derived cardiomyocytes grow up: start young and train harder. *Cell Stem Cell.* (2018) 22:790–1. doi: 10.1016/j.stem.2018.05.011

30. Kuhn B. del Monte F, Hajjar RJ, Chang YS, Lebeche D, Arab S, et al. Periostin induces proliferation of differentiated cardiomyocytes and promotes cardiac repair. *Nat Med.* (2007) 13:962–9. doi: 10.1038/nm1619

31. Liang T, Gao F, Jiang J, Lu YW, Zhang F, Wang Y, et al. Loss of phosphatase and tensin homolog promotes cardiomyocyte proliferation and cardiac repair after myocardial infarction. *Circulation.* (2020) 142:2196–9. doi: 10.1161/CIRCULATIONAHA.120.046372

32. Tseng AS, Engel FB, Keating MT. The GSK-3 inhibitor BIO promotes proliferation in mammalian cardiomyocytes. *Chem Biol.* (2006) 13:957–63. doi: 10.1016/j.chembiol.2006.08.004

33. Zhang L, Zhang Z, Guo H, Wang Y. Na+/K+-ATPase-mediated signal transduction and Na+/K+-ATPase regulation. *Fundam Clin Pharmacol.* (2008) 22:615–21. doi: 10.1111/j.1472-8206.2008.00620.x

34. Grisanti LA. Cardiomyocyte Na(+)/K(+)-ATPase-alpha2 overexpression confers protection in ischemic heart failure. *Am J Physiol Heart Circ Physiol.* (2021) 321:H736–H7. doi: 10.1152/ajpheart.00505.2021

35. Cellini A, Hofler D, Arias-Loza PA, Bandleon S, Langsenlehner T, Kohlhaas M, et al. The alpha2-isoform of the Na(+)/K(+)-ATPase protects against pathological remodeling and beta-adrenergic desensitization after myocardial infarction. *Am J Physiol Heart Circ Physiol.* (2021) 321:H650–H62. doi: 10.1152/ajpheart.00808.2020

36. Gafni J, Munsch JA, Lam TH, Catlin MC, Costa LG, Molinski TF, et al. Xestospongins: potent membrane permeable blockers of the inositol 1,4,5-trisphosphate receptor. *Neuron.* (1997) 19:723–33. doi: 10.1016/S0896-6273(00)80384-0

37. Varghese E, Samuel SM, Sadiq Z, Kubatka P, Liskova A, Benacka J, et al. Anti-cancer agents in proliferation and cell death: the calcium connection. *Int J Mol Sci.* (2019) 20. doi: 10.3390/ijms20123017

38. Pinto MC, Kihara AH, Goulart VA, Tonelli FM, Gomes KN, Ulrich H, et al. Calcium signaling and cell proliferation. *Cell Signal.* (2015) 27:2139–49. doi: 10.1016/j.cellsig.2015.08.006

39. Regulska K, Regulski M, Karolak B, Murias M, Stanisz B. Can cardiovascular drugs support cancer treatment? The rationale for drug repurposing. *Drug Discov Today.* (2019) 24:1059–65. doi: 10.1016/j.drudis.2019.03.010

40. Murata Y, Matsuda T, Tamada K, Hosoi R, Asano S, Takuma K, et al. Ouabain-induced cell proliferation in cultured rat astrocytes. *Jpn J Pharmacol.* (1996) 72:347–53. doi: 10.1254/jjp.72.347

41. Allen JC, Abramowitz J, Koksoy A. Low concentrations of ouabain activate vascular smooth muscle cell proliferation. *Ann N Y Acad Sci.* (2003) 986:504–8. doi: 10.1111/j.1749-6632.2003.tb07235.x

42. Khundmiri SJ, Metzler MA, Ameen M, Amin V, Rane MJ, Delamere NA. Ouabain induces cell proliferation through calcium-dependent phosphorylation of Akt (protein kinase B) in opossum kidney proximal tubule cells. *Am J Physiol Cell Physiol.* (2006) 291:C1247–57. doi: 10.1152/ajpcell.00593.2005

43. Nguyen AN, Jansson K, Sanchez G, Sharma M, Reif GA, Wallace DP, et al. Ouabain activates the Na-K-ATPase signalosome to induce autosomal dominant polycystic kidney disease cell proliferation. *Am J Physiol Renal Physiol.* (2011) 301:F897–906. doi: 10.1152/ajprenal.00095.2011

44. Li J, Zelenin S, Aperia A, Aizman O. Low doses of ouabain protect from serum deprivation-triggered apoptosis and stimulate kidney cell proliferation via activation of NF-kappaB. *J Am Soc Nephrol.* (2006) 17:1848–57. doi: 10.1681/ASN.2005080894

45. Lucas TF, Amaral LS, Porto CS, Quintas LE. Na+/K+-ATPase alpha1 isoform mediates ouabain-induced expression of cyclin D1 and proliferation of rat sertoli cells. *Reproduction.* (2012) 144:737–45. doi: 10.1530/REP-12-0232

46. Tverskoi AM, Sidorenko SV, Klimanova EA, Akimova OA, Smolyaninova LV, Lopina OD, et al. Effects of ouabain on proliferation of human endothelial cells correlate with Na+,K+-ATPase activity and intracellular ratio of Na+ and K. *Biochemistry (Mosc).* (2016) 81:876–83. doi: 10.1134/S00062979160 80083

47. Abramowitz J, Dai C, Hirschi KK, Dmitrieva RI, Doris PA, Liu L, et al. Ouabain- and marinobufagenin-induced proliferation of human umbilical vein smooth muscle cells and a rat vascular smooth muscle cell line, A7r5. *Circulation.* (2003) 108:3048–53. doi: 10.1161/01.CIR.0000101919.00548.86

48. Woo LA, Tkachenko S, Ding M, Plowright AT, Engkvist O, Andersson H, et al. High-content phenotypic assay for proliferation of human iPSC-derived cardiomyocytes identifies L-type calcium channels as targets. *J Mol Cell Cardiol.* (2019) 127:204–14. doi: 10.1016/j.yjmcc.2018.12.015

49. Hotchkiss A, Feridooni T, Zhang F, Pasumarthi KB. The effects of calcium channel blockade on proliferation and differentiation of cardiac progenitor cells. *Cell Calcium.* (2014) 55:238–51. doi: 10.1016/j.ceca.2014.02.018

50. Fan SC Yu BC, Chen ZC, Chen LJ, Chung HH, Cheng JT. The decreased expression of peroxisome proliferator-activated receptors delta (PPARdelta) is reversed by digoxin in the heart of diabetic rats. *Horm Metab Res.* (2010) 42:637–42. doi: 10.1055/s-0030-1253373

51. Chen ZC Yu BC, Chen LJ, Cheng KC, Lin HJ, Cheng JT. Characterization of the mechanisms of the increase in PPARdelta expression induced by digoxin in the heart using the H9c2 cell line. *Br J Pharmacol.* (2011) 163:390–8. doi: 10.1111/j.1476-5381.2011.01212.x

52. Shi H, Mao X, Zhong Y, Liu Y, Zhao X, Yu K, et al. Lanatoside C Promotes Foam Cell Formation and Atherosclerosis. *Sci Rep.* (2016) 6:20154. doi: 10.1038/srep20154

53. Necas J, Bartosikova L, Florian T, Klusakova J, Suchy V, Naggar EM, et al. [Protective effects of the flavonoids osajin and pomiferin on heart ischemia-reperfusion]. *Ceska Slov Farm.* (2006) 55:168–74.

54. Florian T, Necas J, Bartosikova L, Klusakova J, Suchy V, Naggara EB, et al. Effects of prenylated isoflavones osajin and pomiferin in premedication on heart ischemia-reperfusion. *Biomed Pap Med Fac Univ Palacky Olomouc Czech Repub.* (2006) 150:93–100. doi: 10.5507/bp.2006.013

55. Huang SY, Huang GJ, Hsieh PF, Wu HC, Huang WC. Osajin displays potential antiprostate cancer efficacy via impairment of fatty acid synthase and androgen receptor expression. *Prostate.* (2019) 79:1543–52. doi: 10.1002/pros.23876

56. Magadum A, Engel FB. PPARbeta/delta: linking metabolism to regeneration. *Int J Mol Sci.* (2018) 19:2013. doi: 10.3390/ijms19072013

57. Fukuda R, Marin-Juez R, El-Sammak H, Beisaw A, Ramadass R, Kuenne C, et al. Stimulation of glycolysis promotes cardiomyocyte proliferation after injury in adult zebrafish. *EMBO Rep.* 2020:e49752. doi: 10.15252/embr.201949752

58. Burkart EM, Sambandam N, Han X, Gross RW, Courtois M, Gierasch CM, et al. Nuclear receptors PPARbeta/delta and PPARalpha direct distinct metabolic regulatory programs in the mouse heart. *J Clin Invest.* (2007) 117:3930–9. doi: 10.1172/JCI32578

59. Maltsev AV, Kokoz YM, Evdokimovskii EV, Pimenov OY, Reyes S, Alekseev AE. Alpha-2 adrenoceptors and imidazoline receptors in cardiomyocytes mediate counterbalancing effect of agmatine on NO synthesis and intracellular calcium handling. *J Mol Cell Cardiol.* (2014) 68:66–74. doi: 10.1016/j.yjmcc.2013.12.030

60. Lehner Z, Stadlbauer K, Adorjan I, Rustenbeck I, Belz M, Fenzl A, et al. Mechanisms of antihyperglycaemic action of efaroxan in mice: time for reappraisal of alpha2A-adrenergic antagonism in the treatment of type 2 diabetes? *Diabetologia.* (2012) 55:3071–82. doi: 10.1007/s00125-012-2679-x

61. Lamkin DM, Sung HY, Yang GS, David JM, Ma JC, Cole SW, et al. alpha2-Adrenergic blockade mimics the enhancing effect of chronic stress on breast cancer progression. *Psychoneuroendocrinology.* (2015) 51:262–70. doi: 10.1016/j.psyneuen.2014.10.004

62. Mahmoud AI, Kocabas F, Muralidhar SA, Kimura W, Koura AS, Thet S, et al. Meis1 regulates postnatal cardiomyocyte cell cycle arrest. *Nature.* (2013) 497:249–53. doi: 10.1038/nature12054

63. Eulalio A, Mano M, Dal Ferro M, Zentilin L, Sinagra G, Zacchigna S, et al. Functional screening identifies miRNAs inducing cardiac regeneration. *Nature.* (2012) 492:376–81. doi: 10.1038/nature11739

64. Neininger AC, Long JH, Baillargeon SM, Burnette DT, A. simple and flexible high-throughput method for the study of cardiomyocyte proliferation. *Sci Rep.* (2019) 9:15917. doi: 10.1038/s41598-019-52467-0

65. Mills RJ, Parker BL, Quaife-Ryan GA, Voges HK, Needham EJ, Bornot A, et al. Drug screening in human PSC-cardiac organoids identifies pro-proliferative compounds acting via the mevalonate pathway. *Cell Stem Cell.* (2019) 24:895–907 e6. doi: 10.1016/j.stem.2019.03.009

66. Murganti F, Derks W, Baniol M, Simonova I, Trus P, Neumann K, et al. FUCCI-based live imaging platform reveals cell cycle dynamics and identifies pro-proliferative compounds in human iPSC-derived cardiomyocytes. *Front Cardiovasc Med.* (2022) 9:840147. doi: 10.3389/fcvm.2022.840147